The 2010 IEEE/RSJ International Conference on
Intelligent Robots and Systems
October 18-22, 2010, Taipei, Taiwan

Optimal Geometrical Path in 3D with Curvature Constraint

Sikha Hota and Debasish Ghose

Abstract— **This paper presents a path planning approach for achieving an optimal feasible path satisfying a maximum curvature bound in three dimensional space, given initial and final configurations specified by position and orientation vectors. Based on Dubins strategy two types of solution approaches will be discussed, the first is a numerical technique which is computationally intensive and the second is based on 3D geometry from which we will derive an analytical solution. In the second approach, the computational time is very low and the strategy can be implemented for real-time path planning problems. Unlike the existing iterative methods which yield suboptimal paths and are computationally more intensive, this geometrical method generates an optimal path in lesser time. Due to its simplicity and low computational requirements this approach can be implemented on fixed wing aerial vehicles with constrained turn radius.**

I. INTRODUCTION

The shortest path calculation between any two given configurations plays a key role in robotic path planning. In 2D plane, the smooth and shortest path for fixed initial and final configurations is obtained geometrically by Dubins [1]. Reeds and Shepp [2] solve a similar problem using advanced calculus in which a vehicle can move forward as well as backward. Boissonnat et al. [3] prove the same result as Dubins using the powerful Pontryagin's minimum principle. Shkel and Lumelsky [4] classify Dubins path for different sets of initial and final configurations. Using Dubins result in 2D plane optimal path planning is discussed in [5]-[10]. Wong et al. [11] determine C-C-C class of Dubins paths for an Unmanned Air Vehicle (UAV) performing target touring. McGee et al. [12] use Dubins path to explore the problem of finding an optimal path for a UAV in constant wind condition. In [13] Chitsaz et al. consider a problem of finding a time-optimal trajectory for an airplane from some starting point and orientation to some final point and orientation. This model extends the Dubins car to include altitude information and is called a Dubins airplane. It assumes that the system has independent bounded control over the altitude velocity as well as the turn rate of the plane. In [14], [15] the proposed algorithm considers a suboptimal approach to solve the problem of 3D path generation and tracking satisfying arbitrary initial and final conditions. Yang and Sukkarieh [16] present a 3D path planning algorithm for a UAV operating in cluttered natural environments. In [17] Shanmugavel et al. describe coordinated path planning of multiple UAVs in 3D space when the UAVs fly between points which are far apart. In their paper the path planning of UAVs in 2D plane is to 3D space and the suboptimal path of CCSC type (C-Circular, S-Straight line) is generated. By using the Maximum Principle on manifolds Sussmann [18] has shown that every minimizer in 3D is either a helicoidal arc or a concatenation of three pieces each of which is a circle or straight line. An example given in [18] also shows that unlike 2D Dubins path, when the distance between initial and final points is small, there can exist a helicoidal path that is shorter than any CSC path. In [19] and [20], 3D smooth path planning has been discussed using two important properties of 3D curves, curvature and torsion.

In this paper we discuss an efficient algorithm to compute the optimal path with a prescribed curvature constraint in 3D space for a given initial and final configurations under the assumption that the points are situated "sufficiently far" from each other (same as [17]). The condition "sufficiently far" will be clarified in Section III. For this case, the path will be of CSC type and we will construct it using the same principle as of Dubins curve in 2D. Unlike the existing iterative methods which yield suboptimal paths and are computationally more intensive, this geometrical method generates an optimal path in lesser time. Due to its simplicity and low computational requirements this approach can be implemented on a fixed wing aerial vehicle with constrained turn radius.

The organization of the paper is as follows: Section II defines the problem in 3D space. Section III describes the solution approaches. Simulation results are given in Section IV. Finally in Section V concluding remarks are presented.

II. PROBLEM DEFINITION

The problem is to determine a curve of minimum length between the initial point X_1 (X_{1x}, X_{1y}, X_{1z}) and final point X_2 (X_{2x}, X_{2y}, X_{2z}). The orientation vectors at the initial and final points are V_1 (V_{1x}, V_{1y}, V_{1z}) and V_2 (V_{2x}, V_{2y}, V_{2z}), respectively (Fig.1). The problem definition is the same as described by Sussmann [18], where a set of trajectories of a control system Σ have been realized by writing the dynamical equations as

$$\Sigma : x'_p = y_p, \quad y'_p = y_p \times w \tag{1}$$

where, the control w is restricted to taking values in B^3, the close unit ball in R^3; x_p and y_p are the position and velocity vectors, respectively.
The curvature (C) is defined as

$$C = \frac{||x'_p \times y'_p||}{||x'_p||^3}, \quad \text{and} \quad ||C|| \leq C_{max} \tag{2}$$

Sikha Hota is a Research Scholar and Debasish Ghose is a Professor in the Guidance, Control and Decision Systems Laboratory, Department of Aerospace Engineering, Indian Institute of Science, India sikhahota+dghose@aero.iisc.ernet.in

978-1-4244-6676-4/10/$25.00 ©2010 IEEE

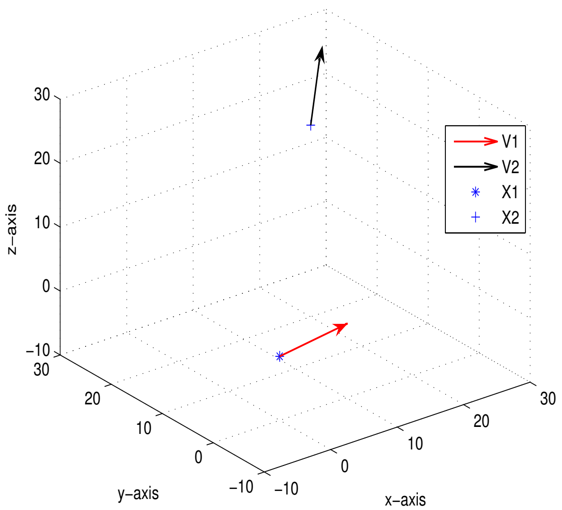

Fig. 1. Problem definition: Initial and final conditions are given in terms of positions and orientations

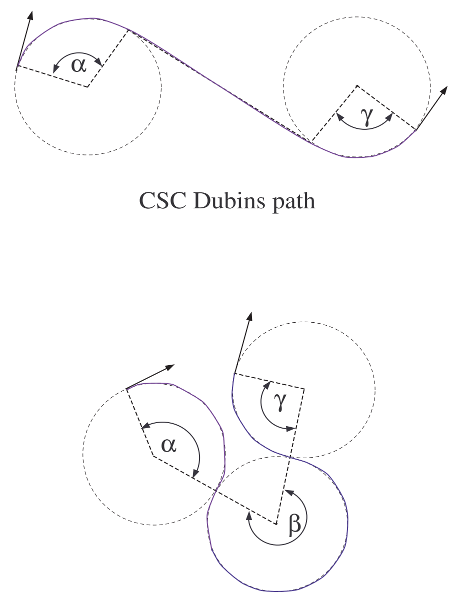

Fig. 2. Dubins CSC and CCC Path in 2D plane

In this paper we will study the construction of optimal path when the initial and final points are "sufficiently far" away from each other.

In two dimensional plane we know that [1] the shortest path for fixed initial and final positions and orientations consists of three consecutive path segments of the Dubins set, D, which includes six paths D={LSL, RSR, RSL, LSR, RLR, LRL} (see Fig. 2), where left turn and right turn with minimal allowed radius of turn are denoted by L and R, respectively, and the straight line path segment is denoted by S. In [4] it was proved that, for this problem, the optimal time path is CSC and not CCC for the long path case. Here C stands for a circular turn either to the right (R) or to the left (L).

Using the same principle as of 2D plane we now attempt to achieve a CSC path in 3D. Unlike the 2D problem the initial and the final manoeuvres are not in the same plane. Hence, the path generation in 3D is not as simple as in the case of 2D. In the following section we will discuss the methods to generate this path.

III. 3D PATH GENERATION

A. Using numerical search approach

In the 2D plane there are only two possible ways of taking a turn (either left or right) when the orientation vector is given. But in 3D there are an infinite number of ways in which a vehicle can turn from its initial orientation and, thus, to reach its final orientation, many possible paths exist. But we have to get a pair of circles, one at the initial and the other at the final position and on which there exists a common tangent. The tangent line between these two circles will give a straight line path segment for the CSC type path.

There are many ways by which a circular path in 3D space can be obtained. We will consider two of them here.

Method 1: Let the radius of the circle be r, the center be (x_a, y_a, z_a) and let (a,b,c) be the unit vector normal to the plane. The equation of the circle can be obtained by considering the intersection of a sphere (of radius r, centered at (x_a, y_a, z_a)) and a plane (passing through (x_a, y_a, z_a) and orthogonal to the vector (a,b,c)). The following equations, parameterized by s, represent the circle.

$$x(s) = x_a + \{acr\cos(s) - br\sin(s)\}/\sqrt{(a^2+b^2)} \quad (3)$$

$$y(s) = y_a + \{bcr\cos(s) + ar\sin(s)\}/\sqrt{(a^2+b^2)} \quad (4)$$

$$z(s) = z_a - r\cos(s)\sqrt{(a^2+b^2)} \quad (5)$$

Method 2: Another way to obtain a circular path is to define two perpendicular unit vectors on the plane of the circle as v and w. If the center of the circle is o, then the equation of the circle, parameterized by γ (which is the angle measured with reference to v) will be,

$$X_s = o + vr\cos\gamma + wr\sin\gamma \quad (6)$$

In the 3D path following problem, the center of the circular turn is not known. Only the position and orientation of initial and final points are known. One can construct the possible turn (see Fig. 3) at initial and final points and a tangent line between these two circles. In other word, a feasible CSC path between these two configurations can be obtained as follows.

Step 1: Obtain the circle on which the centers of all the circles at the initial position are situated. Similarly, obtain the circle on which the centers of all the circles at the final position are situated. This can be achieved by using method

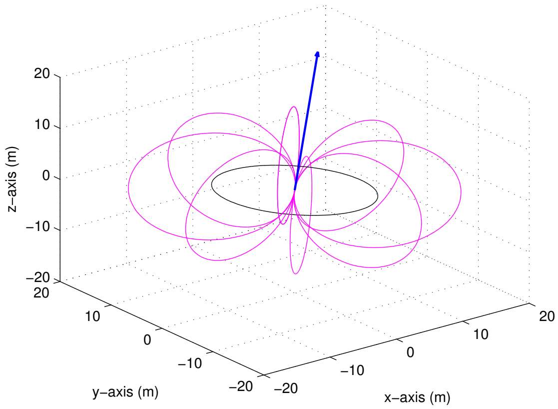

Fig. 3. A figure to illustrate circles formation at a point when the position and orientation vectors are given

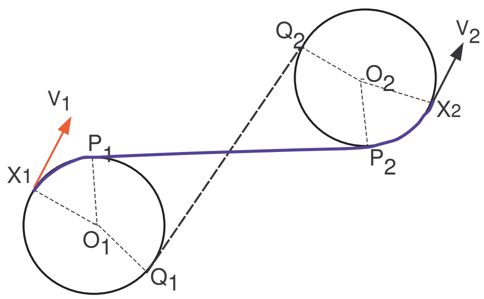

Fig. 4. Illustration of the feasibility of the path

1.
Step 2: Obtain the group of circles which can be the possible turn circles at the initial position. Similarly, obtain the same for the final position. This can be achieved by using method 2.
Step 3: Search a common tangent from these two groups. This common tangent should be along the intersecting line of the initial and the final planes.
Step 4: Check the feasibility of the path. Cross product of the tangent and the radius vector at the tangential point on the first circle should be the same as the cross product of the given initial orientation vector and radius vector at the initial point. Cross product of the tangent and the radius vector at the tangential point on the second circle should be the same as the cross product of the given final orientation vector and radius vector at that final point. In Fig. 4 it is shown that P_1P_2 tangent is a segment of a feasible CSC path whereas Q_1Q_2 is not.
Step 5: Check the minimum length path among all these feasible paths.

B. Using a geometric approach

In this section we will construct the CSC path by using 3D geometry. The intersecting line between the initial and final curve will be derived analytically. The 3D geometry

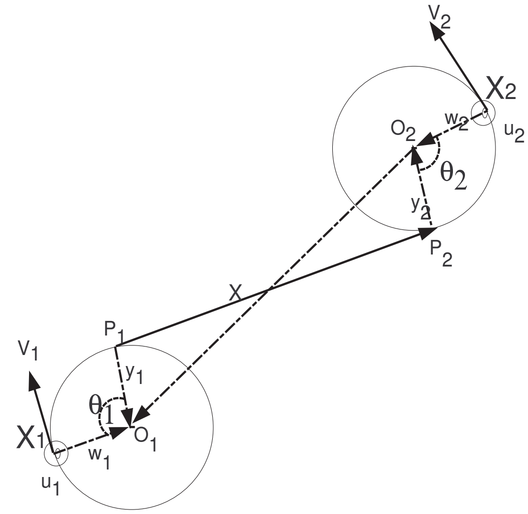

Fig. 5. Geometry of the CSC path in 3D

is shown in Fig. 5. The initial curvilinear path of minimum radius (r) and the final curvilinear path of minimum radius (r) are in different planes. The straight line path segment between these two curves is the intersecting line between these two initial and final maneuver planes. Let the vector that is common for both of these two planes be X (X_x, X_y, X_z). Then, the unit vector x (x_x, x_y, x_z) along this direction is,

$$x = \frac{X}{||X||} \tag{7}$$

The unit orientation vector v_1 (v_{1x}, v_{1y}, v_{1z}) at the initial position is given by,

$$v_1 = \frac{V_1}{||V_1||} \tag{8}$$

The vector perpendicular to the first plane is,

$$U_1 = X \times V_1 \tag{9}$$

Define the unit vector,

$$u_1 = \frac{U_1}{||U_1||} \tag{10}$$

The radius vector that is orientated toward the center of the first circle from its initial position is,

$$W_1 = V_1 \times U_1 = V_1 \times (X \times V_1) \tag{11}$$

Define the unit vector,

$$w_1 = \frac{W_1}{||W_1||} \tag{12}$$

The center of the first circle is

$$o_1 = X_1 + r w_1 \tag{13}$$

Then, the radius vector orientated toward the center of the first circle from the point where the tangent line meets the first circle (this is, the point from which the vehicle will start to follow a straight line path that is tangential to the initial and final circles) is given by,

$$Y_1 = X \times U_1 = X \times (X \times V_1) \tag{14}$$

We define the unit vector,

$$y_1 = \frac{Y_1}{||Y_1||} \tag{15}$$

The point at which the tangent touches the first circle,

$$P_1 = o_1 - ry_1 = X_1 + rw_1 - ry_1 \tag{16}$$

The unit orientation vector v_2 (v_{2x}, v_{2y}, v_{2z}) at the final position is given by,

$$v_2 = \frac{V_2}{||V_2||} \tag{17}$$

The vector perpendicular to the second plane is given by,

$$U_2 = X \times V_2 \tag{18}$$

Define the unit vector,

$$u_2 = \frac{U_2}{||U_2||} \tag{19}$$

The radius vector that is orientated toward the center of the second circle from its final position is given by,

$$W_2 = -V_2 \times U_2 = -V_2 \times (X \times V_2) \tag{20}$$

Define the unit vector,

$$w_2 = \frac{W_2}{||W_2||} \tag{21}$$

The center of the second circle is,

$$o_2 = X_2 + rw_2 \tag{22}$$

Then, the radius vector orientated toward the center of the second circle from the point where the tangent line meets the second circle (this is, the point from which the vehicle will start to follow the second curve) is given by,

$$Y_2 = -X \times U_2 = -X \times (X \times V_2) \tag{23}$$

Define,

$$y_2 = \frac{Y_2}{||Y_2||} \tag{24}$$

Then, the point at which the tangent touches the second circle is,

$$P_2 = o_2 - ry_2 = X_2 + rw_2 - ry_2 \tag{25}$$

We can now solve for X by solving the following nonlinear equation

$$P_2 - P_1 = X \tag{26}$$

We get,

$$X = P_2 - P_1 = (X_2 + rw_2 - ry_2) - (X_1 + rw_1 - ry_1) \tag{27}$$

Let us introduce two new variables θ_1 and θ_2 which are the first and final turning angles, respectively. This will result in the following equation:

$$X = (X_2 - X_1) - r(x + v_1)\tan\frac{\theta_1}{2} - r(x + v_2)\tan\frac{\theta_2}{2} \tag{28}$$

A further simplification will give the following results:

$$\begin{aligned} \cos\theta_1 &= v_1 \,.\, x \qquad (29) \\ \cos\theta_2 &= v_2 \,.\, x \qquad (30) \end{aligned}$$

$$\begin{aligned} (X_{1x} - X_{2x}) = X_x + rx_x &\left[\tan\frac{\theta_1}{2} + \tan\frac{\theta_2}{2}\right] \\ +r&\left[v_{2x}\tan\frac{\theta_2}{2} + v_{1x}\tan\frac{\theta_1}{2}\right] \end{aligned} \tag{31}$$

$$\begin{aligned} (X_{1y} - X_{2y}) = X_y + rx_y &\left[\tan\frac{\theta_1}{2} + \tan\frac{\theta_2}{2}\right] \\ +r&\left[v_{2y}\tan\frac{\theta_2}{2} + v_{1y}\tan\frac{\theta_1}{2}\right] \end{aligned} \tag{32}$$

$$\begin{aligned} (X_{1z} - X_{2z}) = X_z + rx_z &\left[\tan\frac{\theta_1}{2} + \tan\frac{\theta_2}{2}\right] \\ +r&\left[v_{2z}\tan\frac{\theta_2}{2} + v_{1z}\tan\frac{\theta_1}{2}\right] \end{aligned} \tag{33}$$

We can solve these set of equations to get the tangent of these two circles and the angular turns. Now, calculate total length of the path (=first arc length+straight line length+second arc length).
a) First arc length = $r\ \cos^{-1}(w_1.y_1)$.
b) Straight line length = $||P_2 - P_1||$.
c) Second arc length = $r\ \cos^{-1}(w_2.y_2)$.

Note 1: It is important to mention here that there can exist four types of CSC paths (among them we have to select the shortest one) and the solution for those cases can be obtained in the same way as discussed earlier. The complete set of equations are given below.

$$X = (X_2 - X_1) \mp r(x + v_1)\tan\frac{\theta_1}{2} \mp r(x + v_2)\tan\frac{\theta_2}{2} \tag{34}$$

Note 2: From (34) it can be shown that if $||X_2 - X_1|| > 4r$ ("sufficiently far") then all the CSC paths will exist and for smaller distances, the path can be either CSC/CCC or of the helicoidal type. Those cases will not be considered here.

Note 3: The method discussed here gives an optimal geometrical path that may not be flyable for a real UAV with the constraints on flight path angle and stall speed. For example, if final point is just vertically above of the initial point and the orientations are along line-of-sight then although the S path is optimal but it is not flyable. In those cases numerical methods can be applied for obtaining the solution.

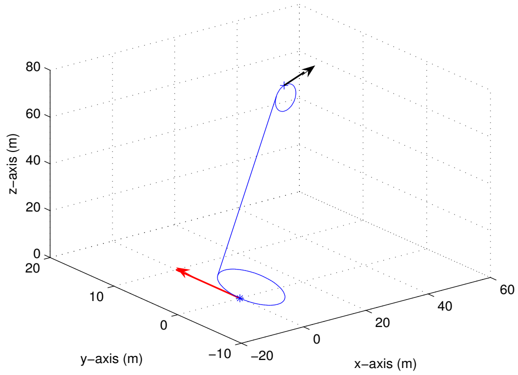

Fig. 6. Case: I

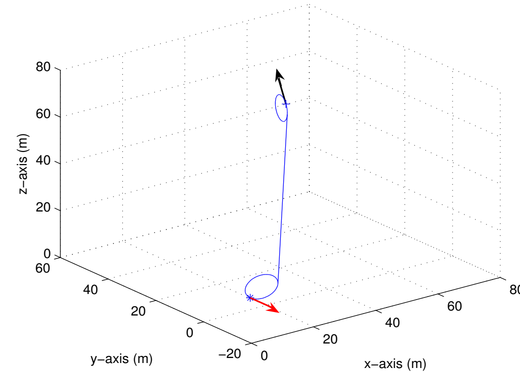

Fig. 8. Case: III

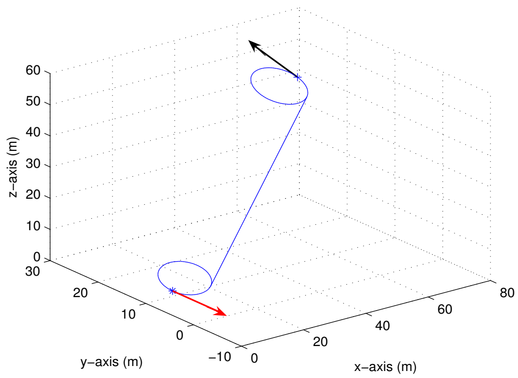

Fig. 7. Case: II

IV. Simulation Results

In Table I, we have taken the same initial conditions as in [17] and the results are tabulated using both numerical and geometrical methods. The value of maximum curvature is .2 (m^{-1}). CSC paths using the geometrical method have been shown in Fig 6-8. In both these methods we will get an optimal path rather than the suboptimal path obtained in [17]. The solution method described in the second case is more efficient in respect to computational time and accuracy (geometry based method takes about 1 sec whereas numerical method takes a minimum of 8 hours with less accuracy) than the method used in [17] which used iterative methods to get the common plane for developing CCSC type suboptimal path. Note that for examples in Table I, the distances between the initial and final points were sufficiently large for a feasible solution of equations (29)-(33) to exist.

V. CONCLUSIONS AND FUTURE WORK

Optimal path planning in 3D space plays a key role in the area of plan planning of an aerial vehicle. In several of the applications, it is crucial to assign paths to each aerial vehicle based on a pre-determined optimal path so that each vehicle can fly from its start point to its ultimate destination through the predefined waypoints in minimum time, reducing the time required to complete the total task. This paper discussed two approaches for obtaining the solution: 1) a numerical method based strategy which is computationally intensive and 2) an approach based on geometry in 3D space from which the analytical solution has been derived. The second method is very effective in providing real time solutions for cases where arbitrary initial and final conditions are given. The proposed method can be implemented for real time 3D path planning as it is computationally fast and it gives the minimum length path to reach the final configuration. Further work in this problem will extend the analysis to cases when the initial position and final position are at close proximity and will consider the implementation of the algorithm using a real UAV model in the presence of wind.

References

[1] L.E. Dubins, "On curves of minimal length with a constraint on average curvature, and with prescribed initial and terminal positions and tangents", *American Journal of Mathematics*, 79 (1957) 497-516.

[2] J.A. Reeds and L.A. Shepp, "Optimal paths for a car that goes both forwards and backwards", *Pacific Journal of Mathematics*, 145 (1990) 367-393.

[3] J.D. Boissonnat, A. Cerezo and J. Leblond, "Shortest paths of bounded curvature constraints", *Journal of Intelligent and Robotic Systems*, 11, No 1-2, 5-20,1994.

[4] A.M. Shkel and V.J. Lumelsky, "Classification of Dubins set", *Robotics and Autonomous Systems*, 34 (2001) 179-202.

[5] G. Yang and V. Kapila, "Optimal path planning for Unmanned Air Vehicles with kinematic and tactical constraints", *Proceedings of the 41st IEEE Conference on Decision and Control*, Las Vegas, NV, 2002, pp. 13011306.

[6] S. Hota and D. Ghose, "Optimal path planning for a miniature air vehicle using a modified Dubins method", *UKIERI Workshop on Robust Control of Smart Autonomous Unmanned Air Vehicle*, Indian Institute of Science, Bangalore, 22-23 August, 2008, pp 64-71.

[7] S. Hota and D. Ghose, "A modified Dubins method for optimal path planning of a miniature air vehicle converging to a straight line path", *Proceedings of the American Control Conference*, St. Louis, Missouri, USA, 10-12 June, 2009.

[8] S. Hota and D. Ghose, "Optimal rectilinear path convergence of a Miniature Air Vehicle using Pontryagin's Maximum Principle", *Proceedings of the International Conference and Exhibition on Aerospace Engineering*, IISc, Bangalore, India, 19-22 May, 2009.

[9] H. Wang, Y. Chen and P. Soueres, "An efficient geometric algorithm to compute time-optimal trajectories for a car-like robot" *Proceedings of the 46th IEEE Conference on Decision and Control*, USA, Dec. 12-14, 2007.

[10] M. Shanmugavel, A. Tsourdos, B.A. White, R. Zbikowski, "Differential Geometric Path Planning of Multiple UAVs" *Journal of Dynamic Systems, Measurement, and Control*, Vol. 129, September 2007.

TABLE I

INITIAL AND FINAL CONDITIONS FOR SIMULATIONS

Case	X_1 (m)	X_2 (m)	v_1	v_2	Numerical Result		Geometrical Result	
					Tangent line(x)	Min. length (m)	Tangent line(x)	Min. length (m)
I	(0,0,0)	(51,18,51)	(0,1,0)	(0,-.3162,.9487)	(0.708,0.202, 0.676)	76.9042	(0.709,0.207,0.674)	76.8888
II	(4,7,5)	(61,18,51)	(0,-1,0)	(0,.9191,.3939)	(0.772, 0.191, 0.606)	79.0666	(.772, 0.190,0.606)	79.0665
III	(15,0,5)	(61,45,51)	(0,-1,0)	(0,.3162,.9487)	(0.544,0.655,0.523)	86.6681	(0.560,0.637, 0.531)	86.6677

[11] H. Wong, V. Kapila, and R. Vaidyanathan, "UAV optimal path planning using C-C-C class paths for target touring", *43rd IEEE Conference on Decision and Control*, December 14-17, 2004, Atlantis, Paradise Island, Bahamas.

[12] T. McGee, S. Spry, and K. Hedrick, "Optimal path planning in a constant wind with a bounded turning rate" *Proc. of the AIAA Guidance, Navigation and Control Conference and Exhibit*, San Francisco, CA, August 2005.

[13] H. Chitsaz and S.M. LaValle, "Time-optimal Paths for a Dubins airplane", *Proceedings of the 46th IEEE Conference on Decision and Control*, New Orleans, LA, USA, Dec. 12-14, 2007

[14] G. Ambrosino, M. Ariola, U. Ciniglio, F. Corraro, A. Pironti and M. Virgilio, "Algorithms for 3D UAV path generation and tracking" *Proceedings of the 45th IEEE Conference on Decision and Control*, San Diego, CA, USA, December 13-15, 2006.

[15] G. Ambrosino, M. Ariola, U. Ciniglio, F. Corraro, E. De Lellis, and A. Pironti, "Path Generation and Tracking in 3-D for UAVs", *IEEE Transactions on Control Systems Technology*, Vol. 17, No. 4, July 2009.

[16] K. Yang, S. Sukkarieh, "3D smooth path planning for a UAV in cluttered natural environments" *Proceedings of the 2008 IEEE/RSJ International Conference on Intelligent Robots and Systems*, Nice, France, Sept, 22-26, 2008.

[17] M. Shanmugavel, A. Tsourdos, R. Zbikowski and B.A. White, "3D Dubins sets based coordinated path planning for swarm of UAVs", *AIAA Guidance, Navigation, and Control Conference and Exhibit*, 21 - 24 August 2006, Keystone, Colorado.

[18] H. J. Sussmann, "Shortest 3-dimensional paths with a prescribed curvature bound" *34th IEEE Conference on Decision and Control*, New Orleans, 1995, pp. 3306-3312

[19] Y. Bestaoui and S. Dicheva "3D Flight Plan for an Autonomous Aircraft" *48th AIAA Aerospace Sciences Meeting Including the New Horizons Forum and Aerospace Exposition* Orlando, Florida, 4 - 7 January 2010.

[20] M. Shanmugavel, A. Tsourdos, R. Zbikowski and B.A. White, "3D path planning for multiple UAVs using Pythagorean Hodograph curves", *AIAA Guidance, Navigation and Control Conference and Exhibit*,Hilton Head, South Carolina, 20 - 23 August 2007.